PART I

Characteristics of Coastal Waves and Currents

CHAPTER 1

On The Characteristics of One-Dimensional Spectra
and Non-Dimensional Parameters of Wind Waves

Toshio Aono*   Chiaki Goto**

Abstract
        Similarity relationship among non-dimensional significant wave
parameters are discussed which is based upon the 3/2 power law. The
characteristics of the wind wave spectra in deep water are investigated by
using the parameters of JONSWAP spectrum and the 3/2 power law. From
theoretical and empirical arguments, it is confirmed that a f^{-4} power law
exists at high frequency range, that JONSWAP spectrum parameter γ and
σ are varied with fetch, and that parameter α and γ satisfied a -1/3 power
law. In shallow water region, spectral form of wind waves is varied with
the shoaling coefficient. Through the analysis of the wind wave spectra, a
new spectral formula is obtained.

1.Introduction
        Relationship between the marine surface wind and wind waves
gives us the basic knowledge in field as diverse as air-sea interaction,
wave hindcasting and engineering design of maritime structures.

        Many researchers pointed out that the frequency spectra of wind-
generated gravity waves shows similarity. It is well known that a similar-
ity law is applicable to the spectral form of wind waves. Phillips (1959)
derived the f^{-5} power law using the similarity and dimensional analysis
argument. Many functional forms of the wind wave spectrum have been
proposed in the past, such as Pierson-Moskowitz (1964), Bretshneider-
Mitsuyasu (1970) and JONSWAP (1973). However, such spectral forms
represent the fully developed condition of wind waves, except the

 *   Senior Research Engineer, Technical Research Institute, Toa
     Corporation, 1-3 Anzen-cho, Tsurumi-ku, Yokohama 230, Japan
 ** Professor, Department of Civil Engineering, Tokai Univ., 1117 Kita-
     kaname, Hiratsuka city, Kanagawa 259-12, Japan

JONSWAP, so that in the case of rapid development of wind waves by typhoon, observed and calculated spectral forms do not show good agreement, especially near the peak frequency. Recently, Toba(1973) derived the f^{-4} power law based on 3/2 power law. This argument of spectral gradient was related to the resistance law between the wind and the wind waves.

These characteristics of wind waves are investigated in deep water, but field observation data is limited at shallow water region, especially under high wave condition. The standard form of shallow water spectrum is proposed by Thornton (1977) and Bouse et. al (1985). These spectrum is based upon the f^{-5} power law.

The present work reveals the quantitative relationship linking marine surface wind and wind waves. The paper discusses the significant wave parameters and the frequency spectrum of wind waves by using the 3/2 power law relation.

2.Observation of wave data

In this study, field observation wave data are used. To get long fetch wave data, 13 wave observation points around the coasts of Japan are used, and to get short fetch wave data, Meteorological station or MT station at Osaka bay is used.

(1) Ocean wind waves

Figure. 1 shows the wave observation system called as NOWPHAS operated by Port and Harbour Research Institute, Ministry of Transport. There are 41 wave observation points. In this study, ocean wave data obtained at 13 major points around the Japan coast are used. These points are located at relatively deep water and there are no topography effects. Table 1 shows the observation systems and
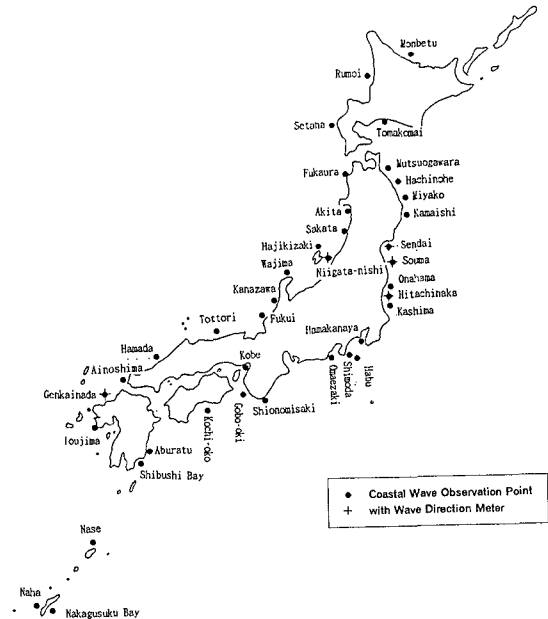

Fig. 1 The NOWPHAS system

Table 1 Observation points

Location	Wavegage Type	Depth(m)	Latitude	Longitude
Hajikizaki	U S W	− 5 4	38° 20'39" N	138° 30'25" W
Wajima Port	U S W	− 5 0	37° 25'40"	136° 54'19"
Fukaura Port	U S W	− 4 9 . 6	40° 39'25"	139° 54'57"
Mutuogawara Port	U S W	− 4 9	40° 55'20"	141° 25'40"
Hitachinaka Port	U S W	− 3 0	36° 23'24"	140° 39'36"
Habu Port	U S W	− 4 9	34° 40'23"	139° 27'18"
Kouchi-oki	A W	− 1 2 0	33° 15'24"	133° 30'06"
Hamada Port	U S W	− 5 1	34° 54'07"	132° 02'21"
Aburatu Port	U S W	− 4 8 . 5	31° 33'27"	131° 26'32"
Setana Port	U S W	− 5 2 . 9	42° 26'30"	139° 49'16"
Monbetu Port	U S W	− 5 2	44° 24'58"	143° 26'00"
Naha Port	U S W	− 5 1	26° 15'19"	127° 38'56"
Nakagusuku Bay	U S W	− 5 0	26° 14'15"	127° 58'10"

condition of each points. The sampling frequency of wave data is 2 Hz. Waves are defined by using the zero up crossing method. Frequency spectra are calculated by using the FFT method. The number of total observation cases are 2546.

These observation points have no wind profile. Thus, a data of the wind waves are determined by using the following criteria.

a) From the time series of significant parameters, significant wave height should be in its developed stage.

b) The swell component is not included in wave data clearly. Thus, a spectral form should be a single peak spectrum.

c) The JONSWAP spectrum parameter γ should be greater than 1.

(2) Wind waves of short fetch

Short fetch waves are obtained at MT station in Osaka Bay. Figure 2 shows the location of MT station. The water depth is 17m. The wave data and wind velocity at 10m high from sea surface are measured at MT station. Sampling frequency is 10 Hz. The analysis method is the same as for ocean waves. The duration of observation used is from 1984 to 1991. The FFT analysis is applied
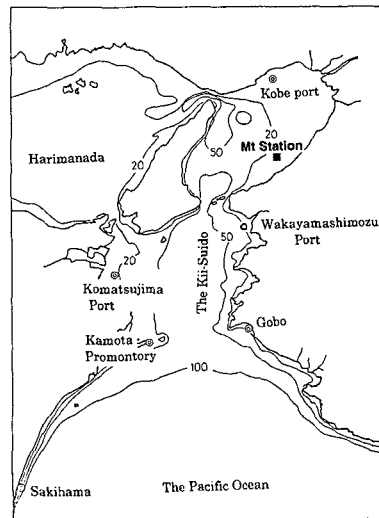

Fig. 2 Location of MT station

to the duration of storm or typhoon. The number of total observation data is 70080 and the data analyzed by FFT is 246.

3. Non-dimensional parameters of wind waves

The non-dimensional parameters that describe the characteristics of wind waves are as follows.

$$\frac{gH_{1/3}}{u_*^2}, \frac{gT_{1/3}}{u_*}, \frac{g^2 E}{u_*^4}, \frac{gF}{u_*^2}, \frac{f_m u_*}{g}, \frac{C}{u_*}, \frac{H_{1/3}}{L_{1/3}} \tag{1}$$

where $H_{1/3}$ is the significant wave height, $T_{1/3}$ the significant wave period, E the wave energy, F the fetch, f_m the peak frequency of spectrum, C the wave celerity, $L_{1/3}$ the wave length corresponding to the significant wave period, u_* the friction velocity of wind, and g the gravity acceleration. Equation (2) is the 3/2 power law relation of Toba (1972):

$$\left(\frac{gH_{1/3}}{u_*^2}\right) = B\left(\frac{gT_{1/3}}{u_*}\right)^{3/2}, B = 0.062 \tag{2}$$

Goto (1990) modified the coefficient B to 0.067. Toba (1992) also showed that if wind waves include components of swell, the exponent of the

Fig. 3 3/2 power law relation

power law is changed from 3/2 to 2. The friction velocity of wind is calculated by using Eq. (3):

$$u_* = \sqrt{C_D} U_{10} \tag{3}$$

where U_{10} is wind speed at a 10m high from the sea surface. To determine the drag coefficient C_D of sea surface, the following Mitsuyasu's formula (1980) is applied:

$$C_D = \begin{cases} (1.290 - 0.024 U_{10}) \times 10^{-3} & (U_{10} < 8m/s) \\ (0.581 + 0.063 U_{10}) \times 10^{-3} & (U_{10} \geq 8m/s) \end{cases} \tag{4}$$

Figure 3 shows the relation of $gH_{1/3}/u_*^2$ and $gT_{1/3}/u_*$ by using the data at MT station. The solid line shows Toba's 3/2 power law while the dotted line shows the Goto's. The deviation of the data from the corresponded line represents the effects of swell components. It is confirmed that the measured wind waves data satisfied the 3/2 power law.

If the relationship linking non-dimensional fetch and energy, significant wave height and wave energy, peak frequency and significant
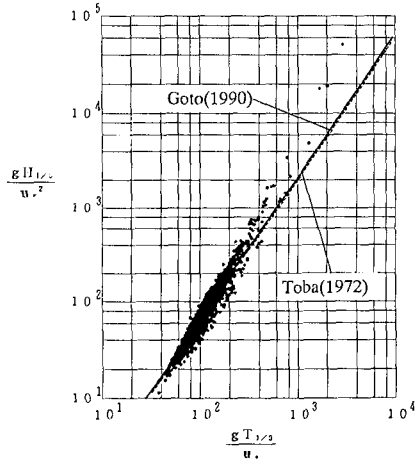
Table 2 Relationship among the non-dimensional parameters
$(Y=\alpha X^n)$

X	gH/U^2		gT/U		g^2E/U^4		gF/U^2		C/U		$f_m U/g$		H/L	
Y	α	n	α	n	α	n	α	n	α	n	α	n	α	n
gH/U^2	1	1	B	$\frac{3}{2}$	a	$\frac{1}{2}$	$aA^{1/2}$	$\frac{1}{2}$	$(2\pi)^{3/2}B$	$\frac{3}{2}$	$\dfrac{B}{b^{3/2}}$	$-\frac{3}{2}$	$(2\pi)^3B^4$	-3
gT/U	$\dfrac{1}{B^{2/3}}$	$\frac{2}{3}$	1	1	$\dfrac{a^{2/3}}{B^{2/3}}$	$\frac{1}{3}$	$\dfrac{a^{2/3}A^{1/3}}{B^{2/3}}$	$\frac{1}{3}$	2π	1	$\dfrac{1}{b}$	-1	$(2\pi)^2B^2$	-2
g^2E/U^4	$\dfrac{1}{a^2}$	2	$\dfrac{B^2}{a^2}$	3	1	1	A	1	$\dfrac{(2\pi)^3B^2}{a^2}$	3	$\dfrac{B^2}{a^2b^3}$	-3	$(2\pi)^6\dfrac{B^8}{a^2}$	-6
gF/U^2	$\dfrac{1}{a^2A}$	2	$\dfrac{B^2}{a^2A}$	3	$\dfrac{1}{A}$	1	1	1	$\dfrac{(2\pi)^3B^2}{a^2A}$	3	$\dfrac{B^2}{b^3a^2A}$	-3	$(2\pi)^6\dfrac{B^8}{a^2A}$	-6
C/U	$\dfrac{1}{2\pi B^{2/3}}$	$\frac{2}{3}$	$\dfrac{1}{2\pi}$	1	$\dfrac{a^{2/3}}{2\pi B^{2/3}}$	$\frac{1}{3}$	$\dfrac{a^{2/3}A^{1/3}}{2\pi B^{2/3}}$	$\frac{1}{3}$	1	1	$\dfrac{1}{2\pi b}$	-1	$2\pi B^2$	-2
$f_m U/g$	$\dfrac{B^{2/3}}{b}$	$-\frac{2}{3}$	$\dfrac{1}{b}$	-1	$\dfrac{B^{2/3}}{ba^{2/3}}$	$-\frac{1}{3}$	$\dfrac{B^{2/3}}{ba^{2/3}A^{1/3}}$	$-\frac{1}{3}$	$\dfrac{1}{2\pi b}$	-1	1	1	$\dfrac{1}{(2\pi)^2bB^2}$	2
H/L	$2\pi B^{4/3}$	$-\frac{1}{3}$	$2\pi B$	$-\frac{1}{2}$	$2\pi\dfrac{B^{4/3}}{a^{1/3}}$	$-\frac{1}{6}$	$2\pi\dfrac{B^{4/3}}{a^{1/3}A^{1/6}}$	$-\frac{1}{6}$	$(2\pi)^{1/2}B$	$-\frac{1}{2}$	$2\pi b^{1/2}B$	$\frac{1}{2}$	1	1

wave period are revealed, all non-dimensional parameter are related to each other by using 3/2 power law.

Table 2 shows the relationship among the non-dimensional parameters. In this table, a is the coefficients of the relationship between wave height and wave energy (Fig. 4), A the coefficients of the relationship between fetch and energy (Fig. 5), b the coefficients of the relationship between peak frequency and wave periods (Fig. 6), and B the coefficient of 3/2 power law. These relation indicate that if the friction velocity and other only one parameter of wind waves are determined, all significant wave parameters can be calculated. The coefficients determine from observed data, are as follows:

$$A = 0.00016, \quad a = 3.86, \quad B = 0.067, \quad b = 1.13 \tag{5}$$
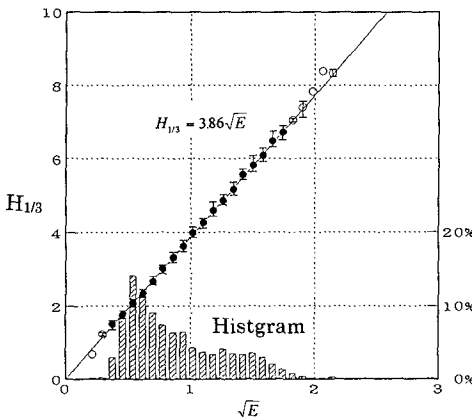

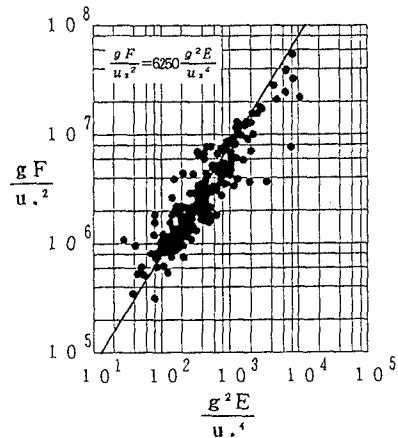Fig. 4 Relationship between $H_{1/3}$ and E

Fig.5 Relationship between E· and F·

Table 3 Comparison between observed and calculated results

X \ Y		gH/u_*^2	gT/u_*	g^2E/u_*^4	gF/u_*^2	C/u_*	$f_m u_*/g$	H/L
gH/u_*^2	observed		0.067	3.86	0.0475	1.0675	0.0628	0.006
	calculated		0.067	3.86	0.0518	1.0552	0.0556	0.005
	ratio		1.	1.	0.9170	1.0117	1.1295	1.2
gT/u_*	observed	6.091		14.97	0.7941	6.281	0.949	0.185
	calculated	6.062		14.91	0.8098	6.283	0.883	0.177
	ratio	1.005		1.004	0.9806	0.999	1.0747	1.0452
g^2E/u_*^4	observed	0.0676	3.10×10^{-4}		1.6×10^{-4}	0.0786	2.74×10^{-4}	1.46×10^{-6}
	calculated	0.0671	3.01×10^{-4}		1.6×10^{-4}	0.0747	2.07×10^{-4}	1.68×10^{-6}
	ratio	1.0075	1.0299			1.0522	1.3237	0.8690
gF/u_*^2	observed	523	2.2267	6250		551	1.9214	0.0136
	calculated	419	1.8830	6250		467	1.2964	0.0105
	ratio	1.25	1.1825	1.		1.18	1.4821	1.2952
C/u_*	observed	0.9696	0.1592	2.3840	0.1264		0.1510	0.0295
	calculated	0.9648	0.1590	2.3741	0.1289		0.1405	0.0282
	ratio	1.0050	1.0013	1.0042	0.9806		1.0747	1.0461
$f_m u_*/g$	observed	0.1575	0.9489	0.0640	1.2191	0.1511		5.6241
	calculated	0.1457	0.8830	0.0592	1.1289	0.1405		4.9829
	ratio	1.0810	1.0746	1.0811	1.1180	1.0754		1.1287
H/L	observed	0.1745	0.4259	0.1113	0.4755	0.1700	0.4377	
	calculated	0.1710	0.4210	0.1090	0.4678	0.1679	0.4480	
	ratio	1.0205	1.0116	1.0211	1.0165	1.0125	0.9770	

Table 3 shows the comparison between observed and calculated results. The results show good agreement. Thus, table 2 shows similarity of wind waves parameter.

4. Wave spectrum in deep and shallow water

On the basis of the non-dimensional significant wave parameter, frequency spectra of wind waves in the deep and shallow water region are discussed and a new functional form of wind wave spectrum is proposed.

The JONSWAP spectrum is an extension form of Pierson-Moskowitz spectrum and is applicable to cases ranging from developing wave to fully developed wave. Equation (6) is the generalized JONSWAP spectrum.

Fig. 6 Relationship between f_m^* and $T_{1/3}$

$$S(f) = \alpha (2\pi)^{-m+1} g u_*^{5-m} f^{-m} \exp\left\{ -\frac{m}{4}\left(\frac{f}{f_m}\right)^{-4} \right\} \gamma^{\beta}$$

$$\beta = \exp\left\{ -(1 - f/f_m)^2 / 2\sigma^2 \right\}$$

(6)

where α is scale factor, γ the peak enhancement factor, σ the band width near peak frequency. By using this equation, the similarity and the characteristics of slope of high frequencies and parameter of spectrum are dis-
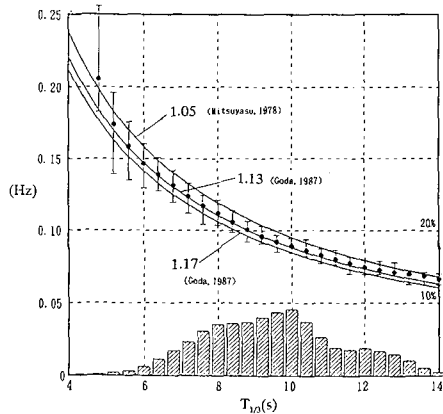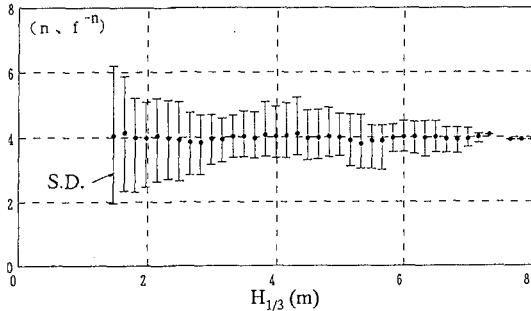
cussed.

Figure 7 shows the slope of wind wave spectra at high frequencies by using least-squares estimation. The high frequency range is the same as Donelan's (1985). The x-axis is significant wave height. In this figure, the vertical lines are the standard deviations of the data to

Fig. 7 Slope of the spectrum in high frequency range

indicate the amount of scatter. From Fig. 7 , the mean slope of wind wave spectra at high-frequency range is approximated by f^{-4} power law. The amount of scatter decreases with increasing wave height. This fact implies that the 3/2 power law is applicable in the frequency domain and the development of the wind waves is essentially a strongly nonlinear phenomenon. Hence, the JONSWAP spectrum follows the f^{-4} law, expressed as follows:

$$S(f) = \alpha(2\pi)^{-3} g u_* f^{-4} \exp\left\{-(f/f_m)^{-4}\right\} \gamma^{\beta} \tag{7}$$

The functional forms of the peak enhancement factor γ are proposed by Donelan (1985) and Mitsuyasu (1980). They use the non-dimensional peak frequency as variable. Figure 8 shows the relationship linking γ and non-dimensional peak frequency $f_{m*}=f_m u_*/g$. The vertical lines are standard deviations. There is a large scatter in γ, but the mean value is increasing with non-dimensional peak frequency and has log-linear relation. It means the spectral form is change to Pierson-Moskowitz spectrum with the increase of the fetch. Hence, the following empirical formula for γ is obtained:

$$\gamma = 6 f_{m*}^{0.15} \tag{8}$$

The scale factor α is varied with spectral form. In this study, the relationship between α and γ is discussed. The total energy of JONSWAP spectrum is
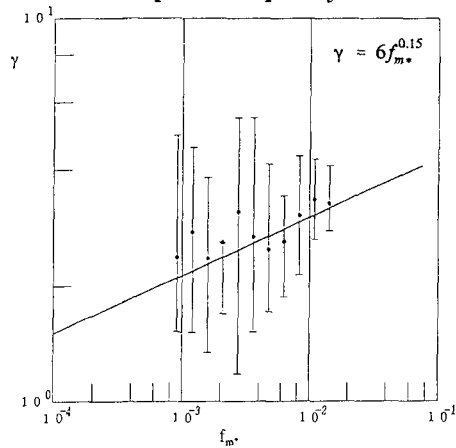

Fig. 8 Relationship between γ and f_{m*}

$$E = \alpha (2\pi)^{-3} g u_* f_m^{-4} M_0 \tag{9}$$

where, M_0 is expressed as Eq. (10)

$$M_0 = \int_0^{\infty} \left(\frac{f}{f_m}\right)^{-4} \exp\left\{-\left(\frac{f}{f_m}\right)^{-4}\right\} \gamma^{\beta} df \tag{10}$$

therefore, M_0 is approximated by (Goto and Aono, 1993)

$$M_0 = 0.30 \gamma^{1/3} \tag{11}$$

By using this approximate formula for M_0 and the relation of non-dimensional energy and peak frequency, and the 3/2 power law, this equation is derived:

$$\alpha \approx \gamma^{-1/3} \tag{12}$$

From Eq. (12), α is related to γ. Table 4 shows the relationship linking α and γ derived using the 3/2 power law for various spectral forms.

Table 4 Relationship between α and γ

Power	Pierson·Moskowitz	JONSWAP
-4	C o n s t.	$\alpha \sim \gamma^{-1/3}$
-5	$\alpha \sim \left[\dfrac{g^2 E}{u_*^4}\right]^{-1/3}$	$\alpha \sim \gamma^{-1/3}\left[\dfrac{g^2 E}{u_*^4}\right]^{-1/3}$

Figure 9 shows the relation of α and γ, while solid line correspond to the least squares estimate. The coefficient is determined from the line and yields

$$\alpha = 0.17 \gamma^{-1/3}. \tag{13}$$

Figure 10 and Fig. 11 show the relation of σ_1, σ_2, and the non-dimensional peak frequency. The symbol σ_1 is low frequency side while σ_2 is high frequency side. Because the low frequency side include the weak swell components, there are no trends in σ_1. In the high frequency side, σ_2 varies inversely as the non-dimensional frequency on a log-log axis. This means the spectral form near peak frequency is varied from sharp to mild in the case of developing wind waves. Hence the band width near peak frequency is determined:
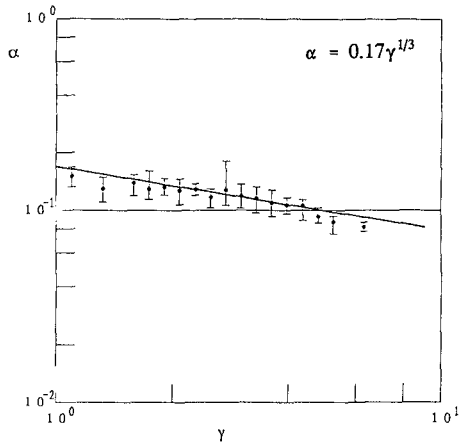

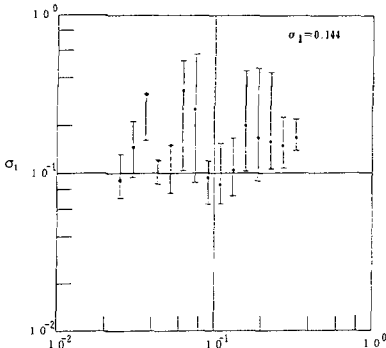Fig. 9 Relation between α and γ
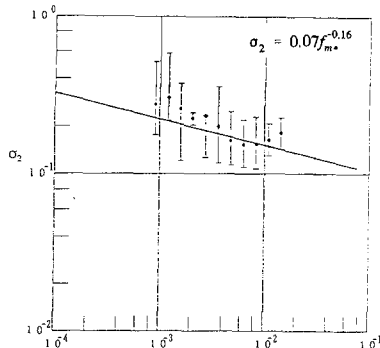
Fig. 10 Relation of σ_1 and f_{m*}

Fig. 11 Relation of σ_2 and f_{m*}

$$\sigma_1 = 0.144, \qquad \sigma_2 = 0.07 f_{m*}^{-0.16} \tag{14}$$

These characteristics of spectral parameters are in deep water region. Next, the spectrum in shallow water region is discussed.

Figure 12 show the change of the coefficient of 3/2 power law in shallow water. The x-axis is relative depth, the shaded bar is the histogram of observed data and the solid line is the linear shoaling coefficient Ks. The mean value of B/B_0 shows good agreement with Ks. The 3/2 power

Fig. 12 Relation of B and h/L_0

law is also extended in a shallow water region by using the shoaling coefficient.
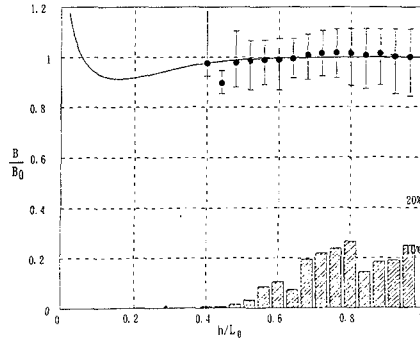
The spectral form in shallow water is derived by using 3/2 power law. In this derivation, subscript 0 indicates values in deep water and s indicates there in shallow water. The integrated form of the JONSWAP spectrum is

$$E_0 = \alpha_0 g u_* f_m^{-3} M_1 \tag{15}$$

where M_1 is

$$M_1 = \int_0^\infty \left(\frac{f}{f_m}\right)^{-4} \exp\left\{-\left(\frac{f}{f_m}\right)^{-4}\right\} \gamma_0^\beta \, d\left(\frac{f}{f_m}\right). \tag{16}$$

From the analogy of M_0, M_1 is approximated by Eq. (17)

$$M_1 = c\gamma_0^{1/3} \tag{17}$$

Thus, Eq. (15) is expressed as

$$E_0 = c\alpha_0 u_* \gamma_0^{1/3} f_m^{-3} \tag{18}$$

Using the relationship of $u_* f_m/g$ and gT_0/u_* and the relationship of gH_0/u_*^2 and $g^2 E_0/u_*^4$, Eq. (19) is derived.

$$\left[\frac{gH_0}{u_*^2}\right] = a\left[\alpha_0 b^{-3} c\gamma_0^{1/3}\right]^{1/2} \left[\frac{gT_0}{u_*}\right]^{3/2} \tag{19}$$

Equation (19) is the 3/2 power law which derived from the spectral form. The coefficient B_0 of 3/2 power law in deep water region is expressed as Eq. (20).

$$B_0 = \left[ab^{-3/2}\right]\left[\alpha_0 c\gamma_0^{1/3}\right]^{1/2} \tag{20}$$

If the coefficients a, b and B_0 is constant, the relationship between α_0 and γ_0 is

$$\alpha_0 = \left[\frac{B^2}{ab^{-3}}\right]\frac{1}{c\gamma_0^{1/3}} \tag{21}$$

The same argument applies in shallow water. The total energy and the coefficient of 3/2 power law in shallow water is expressed by the following equations:

$$E_s = c\alpha_s \gamma_s^{1/3} u_* f_m^{-3} \tag{22}$$

$$\left[\frac{gH_s}{u_*^2}\right] = a\left[\alpha_s b^{-3} c\gamma_s^{1/3}\right]^{1/2} \left[\frac{gT_s}{u_*}\right]^{3/2} \tag{23}$$

The coefficient of 3/2 power law is

$$B_s = B_0 K_s = a\left[\alpha_s b^{-3} c\gamma_s^{1/3}\right]^{1/2} \tag{24}$$

The combination of Eq. (20) and Eq. (24) lead to Eq. (25).

$$\left[\frac{\gamma_s}{\gamma_0}\right]^{1/6} = K_s \qquad \alpha_0 = \alpha_s \tag{25}$$

Equation (25) determine the spectral form in shallow water. **Figure 13** shows the change of γ with relative depth h/L_0. The mean value of γ and K_s show good agreement.

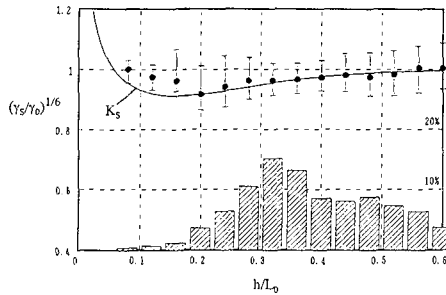The characteristics of the wind waves spectrum in deep water are invest-
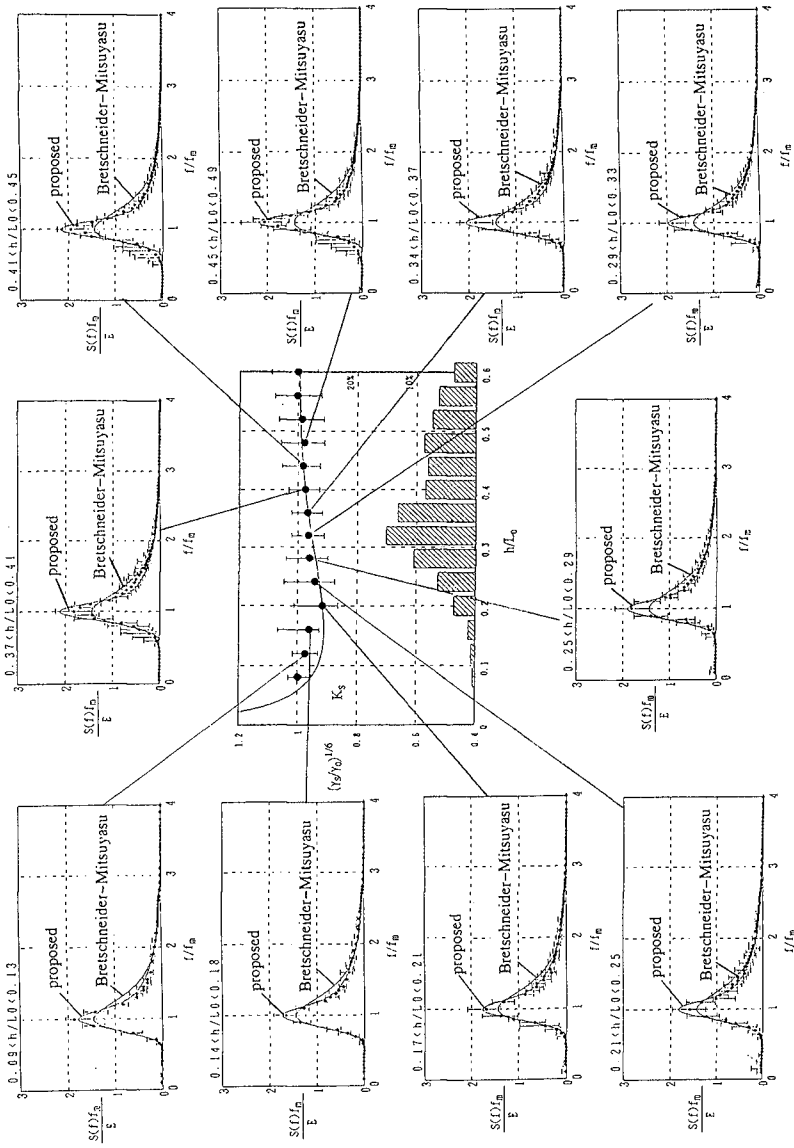

Fig. 13 Change of γ with h/L_0.

Fig. 14 Change of the spectral form with h/Lo.

gated by using the parameters of JONSWAP spectrum. From theoretical and empirical arguments, it is confirmed that a f^{-4} power law exists at high frequency range, that γ and σ are varied with fetch, and that a $-1/3$ power law, based on $3/2$ power law, also exists in relation between α and γ. Wave energy is concentrated near the peak frequency during the development stage, and approaches the Pierson-Moskowitz spectrum gradually with the increase of fetch. In shallow water region, the spectral form of wind waves varies with the shoaling coefficient. From these characteristics of the wind wave spectrum, the following new spectral formula is obtained:

$$\left.\begin{array}{l} S(f) = \alpha(2\pi)^{-3} g u_* f^{-4} \exp\left[-(f/f_m)^{-4}\right] \gamma^{\beta} \\[2mm] \beta = \exp\left[1 - (f/f_m)^2 / 2\sigma^2\right] \end{array}\right\} \tag{26}$$

$$\left.\begin{array}{l} \gamma = 6 f_{m*}^{0.15}, \quad \alpha = 0.17\gamma^{-1/3}, \quad f_m = 1/1.136 T_{1/3} \\[2mm] \sigma_1 = 0.144, \quad \sigma_2 = 0.07 f_{m*}^{-0.16}, \quad f_{m*} = f_m u_* / g \\[2mm] u_* = H_{1/3}^2 / g B^2 T_{1/3}, \qquad B = 0.067 \end{array}\right\} \tag{27}$$

In shallow water region, the spectral form of wind waves is expressed as

$$S_s(f) = K_s^{6\beta} S(f) \tag{28}$$

In this spectrum, the input variables are significant wave height and period only. Figure 14 shows the comparison of the newly-proposed spectral model with the observed spectral data and Bretshneider-Mitsuyasu spectrum. The spectral form varies with h/L_0 and the proposed model and observed data show good agreement.

5. Discussion

Table 4 shows the relationship between non-dimensional wave height and period derived from selected spectral forms. Where B is coefficients and β_1 is power. It is confirmed that $3/2$ power law relation applies to f^{-4} power law and 2 power law relation applies to f^{-5} power law. 2 power law relation is revealed under the condition that the swell components are included in the wind waves. This is the reason of such change of power.

Table 4 Relationship between H* and T* derived from spectral forms.

Power	Pierson·Moskowitz		JONSWAP	
	B	$\beta 1$	B	$\beta 1$
-5	$a\, b^{-2}[0.2\alpha]^{1/2}$	2	$a\, b^{-2}[0.2\alpha\, \gamma^{1/3}]^{1/2}$	2
-4	$0.5a[\alpha\, b^{-3}]^{1/2}$	$3/2$	$a[\alpha\, b^{-3} c\, \gamma^m]^{1/2}$	$3/2$

The 3/2 power law is not dependent on the fetch and shows local equilibrium between wind and wind waves. In the frequency domain, such local equilibrium is revealed by the f^{-4} power law. It implies that the spectral form depends on the characteristics of the high frequency range. However, spectral parameters depend on the fetch, so that the spectral form cannot be determined from the 3/2 power law directly. The implication in the case of developing wind waves is that α varies with γ, which depends on the fetch, in order to satisfy the 3/2 power law.

To apply Eq. (28) for actual work, it is necessary to investigate the error between the observed data and Eq. (28). The error of the calculated spectrum is defined as

$$E_r = \frac{\int_0^\infty |S_c(f) - S_o(f)| df}{\int_0^\infty S_c(f) df} \quad (29)$$

Figure 15 shows the characteristics of the error of proposed spectrum and Bretschneider-Mitsuyasu spectrum. The horizontal axis is the U_{10} calculated by using the 3/2 power law and Mitsuyasu's C_D law. The error of the proposed spectrum is relatively small in 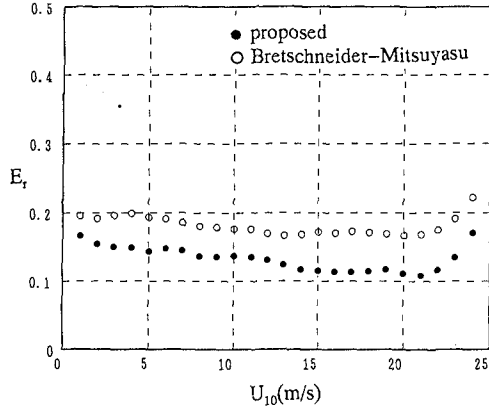the entire range of wind velocity. The error is being large in the range of low wind velocity and the wind velocity is greater than the 22m/s. These characteristics of error indicates the mixture of wind waves and swell at low wind velocity range. The increase of error at high wind velocity range suggest the change of the wind resistance law, but there is not enough the data such high wind velocity range.

Fig. 15 Error of the spectrum

Figure 16 shows the results of comparison of the observed and proposed spectra. The spectrum of Bretschneider-Mitsuyasu is given in this figure for reference. Observation data was taken from Kochi-Oki on July, 1981. Time series of $H_{1/3}$, $T_{1/3}$, h/L_0, and error which defined by Eq. (29) is also shown in Fig. 16. It can be seen that the proposed spectrum shape agrees well with the observed one.

6. Conclusions
       The major conclusions of this study are as follows:
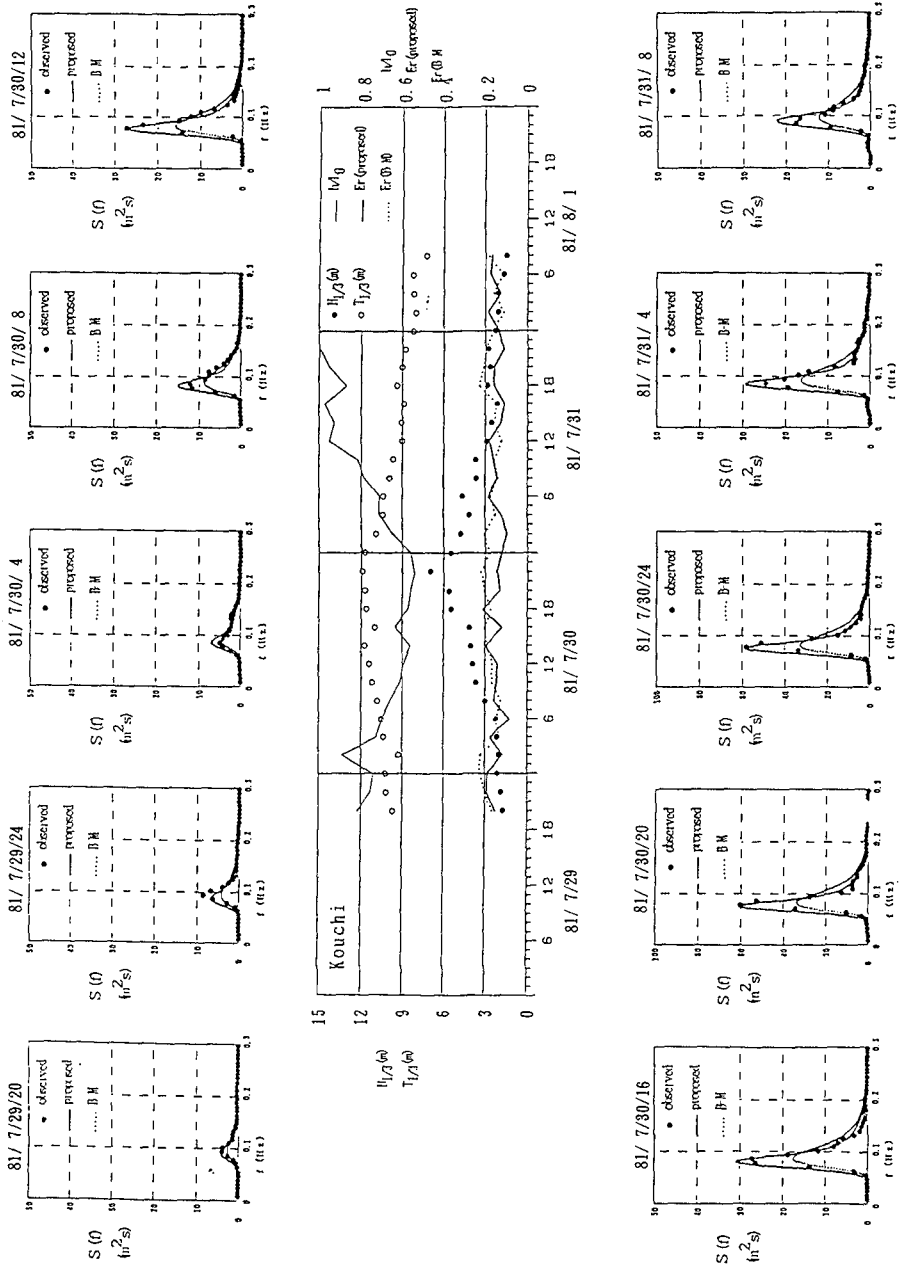(1) It was confirmed that the measured wind waves data satisfied the 3/2

Fig. 16 Results of the comparison of the observed and proposed spectra.

power law which is an empirical formula between non-dimensional wave height and period.

(2) By using the 3/2 power law relation, non-dimensional parameters of wind waves are all related.

(3) The new spectral model, which is based on the 3/2 power law, is proposed. This spectral model is evaluated from $H_{1/3}$ and $T_{1/3}$, and calculated result is very accurate. The applicability of this new spectrum is very wide, ranging from the case of developing wind to that of fully developed wind, and from deep to shallow water region.

Reference

(1) Bouws, E., H. Gunther, W. Rosenthal and C. L. Vincent (1985): Similarity of the wind wave spectrum in finite depth water 1.Spectral form, J. Geophys. Res., Vol.90 No.C1, pp.975-986.

(2) Donelan, M.A., J. Hamilton and W. H. Hui (1985): Directional spectra of wind-generated waves, Phil. Trans. R. Soc. Lond. A315,pp.509-562.

(3) Ebuchi, N., Y. Toba and H. Kawamura (1992): Statistical study on the local equilibrium between wind and wind waves by using data from ocean data buoy stations, J. Oceanogr., Vol.48, pp.77-92.

(4) Goto, C., K. Suetsugu and T. Nagai (1990): Wave Hindcast Model for Short Fetch Sea, Rep. of P.H.R.I. Vol.29, No.3, pp. 3-26.

(5) Goto, C. and T. Aono (1993) : On the Characteristics of One-Dimensional Spectra and Non-Dimensional Parameters of Wind Waves - Wave Hindcast Model Using the Hybrid-parameter Methods (2nd report) -, Rep. of P.H.R.I, Vol. 32, No.1, pp. 53-99 (in Japanese)

(6) Hasselman, K. et. al(1973):Measurements of wind wave growth and swell decay during the Joint North Sea Wave Project (JONSWAP), Deut. Hydrgr. Z.,Suppl. 8, pp.1-95.

(7) Mitsuyasu, H (1968): On the growth of the spectrum of wind generated waves (1), Rep. Res. Inst. Mech. Kyushu Univ., Vol.16, pp.459-482.

(8) Mitsuyasu, H., R. Nakamura and T. Komori (1971): Observation of the wind and waves in Hakata Bay, Rep. Res. Inst. Mech. Kyushu Univ., Vol.19, pp.37-74.

(9) Phillips, O. M. (1958): The equilibrium range in the spectrum of wind-generated waves, J. Fluid Mech., 4, pp. 426-434.

(10) Pierson, W. J. and L. Moskowitz (1964): A proposed spectral form for fully developed wind seas based on the similarity theory of S. A. Kitaigorodskii, J. Geophys. Res., 69, pp.5181-5190.

(11) Thornton, E. B. (1977): Rederivation of the saturation range in the frequency spectrum of wind-generated gravity waves, J. Phys. Oceanogr., Vol.7, pp.137-140.

(12) Toba, Y. (1972): Local balance in the air-sea boundary processes, I. On the growth process of wind waves, J. Oceanogr Soc. Japan, 28, pp. 109-120.

(13) Toba, Y. (1973): Local balance in the air-sea boundary processes, III. On the spectrum of wind waves, J. Oceanogr. Soc. Japan, 29, pp. 209-220.